

# Constraining the density dependence of symmetry energy from nuclear masses

B. K. Agrawal<sup>1</sup>, J. N. De<sup>1</sup>, S. K. Samaddar<sup>1</sup>, G. Colò<sup>2,3</sup>, and A. Sulaksono<sup>4</sup>

<sup>1</sup> *Saha Institute of Nuclear Physics, Kolkata 700064, India*

<sup>2</sup> *Dipartimento di Fisica, Università degli Studi di Milano, via Celoria 16, I-20133 Milano, Italy*

<sup>3</sup> *INFN, sezione di Milano, via Celoria 16, I-20133 Milano, Italy*

<sup>4</sup> *Departemen Fisika, FMIPA, Universitas Indonesia, Depok 16424, Indonesia*

Empirically determined values of the nuclear volume and surface symmetry energy coefficients from nuclear masses are expressed in terms of density distributions of nucleons in heavy nuclei in the local density approximation. This is then used to extract the value of the symmetry energy slope parameter  $L$ . The density distributions in both spherical and well deformed nuclei calculated within microscopic framework with different energy density functionals give  $L = 59.0 \pm 13.0$  MeV. Application of the method also helps in a precision determination of the neutron skin thickness of nuclei that are difficult to measure accurately.

PACS numbers: 21.65.Ef, 21.65.Mn, 21.10.Gv

Keywords: Symmetry energy, symmetry energy slope parameter, nuclear matter, neutron skin

The nuclear symmetry energy measures the energy transfer in converting symmetric nuclear matter to the asymmetric one. The density dependence gives information on the isospin-dependent part of the equation of state (EOS) of asymmetric nuclear matter. The density content of symmetry energy is mostly encoded in the symmetry energy coefficient  $C_v$ , the symmetry slope parameter  $L$  and the symmetry incompressibility  $K_{sym}$ , all evaluated at the nuclear saturation density  $\rho_0$ . Here  $C_v(\rho)$  is the volume symmetry energy per nucleon of homogeneous nuclear matter at density  $\rho$ ,

$$C_v(\rho) = [e(\rho, X = 1) - e(\rho, X = 0)], \quad (1)$$

$$L = 3\rho_0 \left. \frac{\partial C_v(\rho)}{\partial \rho} \right|_{\rho_0}, \quad (2)$$

and

$$K_{sym} = 9\rho_0^2 \left. \frac{\partial^2 C_v(\rho)}{\partial \rho^2} \right|_{\rho_0}. \quad (3)$$

In Eq. (1),  $e$  is the energy per nucleon and  $X = (\rho_n - \rho_p)/(\rho_n + \rho_p)$  is the isospin asymmetry of the system. The parameters  $C_v(\rho_0)$ ,  $L$  and  $K_{sym}$  deem to be of fundamental importance in both nuclear physics and astrophysics. The nuclear binding energies, the position of the nuclear drip lines, the neutron skin thickness or the neutron density distribution in neutron-rich nuclei, – all of these are known to have affectations from [1–8] the symmetry parameters so mentioned. Many astrophysical phenomena also depend sensitively on the symmetry slope parameter  $L$ . Most notable among them are the dynamical evolution of the core collapse of a massive star and the associated explosive nucleosynthesis [9, 10], the cooling of proto-neutron stars through neutrino convection [11] or the radii of cold neutron stars [11]. The nature and stability of phases within a neutron star, its crustal com-

[12] also seem to be strongly influenced by the symmetry energy and its density dependence. A glimmer of their import could further be seen in relation to some issues of new physics beyond the standard model [13, 14].

Attempts on estimates of  $L$  have been made in the last few years from analyses of diverse experimental data, uncertainties still linger, however. Pygmy dipole resonance [15] in  $^{68}\text{Ni}$  and  $^{132}\text{Sn}$  predicts a weighted average in the range  $L = 64.8 \pm 15.7$  MeV, but giant dipole resonance in  $^{208}\text{Pb}$  [16] points to a value of  $L \sim 52 \pm 7$  MeV. Nucleon emission ratios from heavy ion collisions [17] favor a value close to it,  $L \sim 55$  MeV, but isoscaling gives  $L \sim 65$  MeV [18] and isospin diffusion shifts the value further up,  $L = 88 \pm 25$  MeV [19, 20]. Recently, analyzing nuclear energies within the standard Skyrme-Hartree-Fock approach, Chen [21] brought down  $L$  to  $52.5 \pm 20$  MeV. However, from the fit [3] of the experimental nuclear masses to the calculated ones in the finite range droplet model, the value of  $L$  is found to be in the bound  $L = 70 \pm 15$  MeV. Inputs from astrophysical analyses, namely neutron star masses and radii on the other hand constrain  $L$  to  $43 < L < 52$  MeV [22].

The neutron skin thickness  $R_{skin}$  ( $=R_n - R_p$ ;  $R_n$  and  $R_p$  are the neutron and proton root-mean squared (rms) radii) of  $^{208}\text{Pb}$  calculated in the droplet model or in self-consistent quantal calculations with many different interactions was found to have a strong linear correlation with the density dependence of symmetry energy around saturation [4–7, 23, 24]. Analyzing the correlation systematics of nuclear isospin with neutron skin thickness for a series of nuclei in the ambit of droplet model, the Barcelona Group [23, 24] found a range for as  $L = 75 \pm 25$  MeV. The neutron skin thicknesses used by them are measured in antiprotonic atom experiments [25, 26], they carry the unavoidable strong interaction-related uncertainties. This had its imprint on their extracted value of  $L$ . The Lead Radius Experiment on Pb (PREX) promises a model-independent probe of its neutron-skin

put the value of  $R_{skin}$  of  $^{208}\text{Pb}$  in more precision than  $0.302 \pm 0.175$  fm [27, 28]. This large uncertainty mires  $L$  in wide limits.

Given that the neutron skin thickness is a strong indicator of the nuclear isovector properties, the nuclear dipole polarizability  $\alpha_D$  has been suggested to provide a unique constraint on  $R_{skin}$  [29, 30]. The recent high resolution ( $p, p'$ ) measurement [31] of  $\alpha_D$  yields the neutron skin thickness of  $^{208}\text{Pb}$  to be  $0.168 \pm 0.022$  fm [32]. Quadrupole resonance energies may similarly be exploited to give estimates of  $R_{skin}$ . Microscopic calculations [33] of these observables based on families of non relativistic and covariant energy density functionals (EDF) point to a value of  $R_{skin}$  in close vicinity,  $R_{skin} = 0.14 \pm 0.03$  fm for  $^{208}\text{Pb}$ . Consequently, value of the symmetry slope parameter extracted from the GDR and GQR measurements turns out to be  $L = 49 \pm 11$  and  $37 \pm 18$  MeV, respectively.

Nuclear masses are one of the most precisely experimentally determined quantities in nuclear physics. They provide information, through the liquid-drop mass systematics on the values of the volume and surface symmetry energy coefficients  $C_v(\rho_0)$  and  $C_s$ . The symmetry energy coefficient,  $a_{sym}(A)$ , for a nucleus with mass number  $A$  can be expressed in terms of  $C_v(\rho_0)$  and  $C_s$  as,

$$a_{sym}(A) = C_v(\rho_0) - C_s A^{-1/3}. \quad (4)$$

An alternative form for  $a_{sym}(A)$  has also been suggested [34], namely,

$$a_{sym}(A) = \frac{C_v(\rho_0)}{(1 + \kappa A^{-1/3})^\gamma}, \quad (5)$$

where  $\kappa = C_s/C_v(\rho_0)$ . From analyses of  $\sim 2000$  nuclear masses, Liu *et al.* [35] obtained  $C_v(\rho_0) = 31.1 \pm 1.7$  MeV and  $\kappa = 2.31 \pm 0.38$ . Equating  $a_{sym}(A)$  with  $C_v(\rho_A)$ , where  $\rho_A$  is an equivalent density specific to mass  $A$  and taking an ansatz for the density dependence of  $C_v(\rho)$  as

$$C_v(\rho) = C_v(\rho_0) \left(\frac{\rho}{\rho_0}\right)^\gamma, \quad (6)$$

they obtain, choosing  $\rho_A \sim 0.1$  fm $^{-3}$  for  $^{208}\text{Pb}$ ,  $\gamma = 0.7 \pm 0.1$  and thence  $L = 66 \pm 13$  MeV. The density dependence of  $C_v$  as given by Eq. (6) is quite consistent with the density dependence obtained from the nuclear EOS with different interactions [17–20, 36]; the value of  $\gamma$  varies though from interaction to interaction. The choice for the value of the equivalent density has no firm theoretical basis, however.

A meticulous study [37] of the double differences of 'experimental' symmetry energies were done very recently. The double differences in symmetry energies of neighboring nuclei has the advantage that effects from pairing and shell corrections are well canceled out, resulting in a compact correlation between the double differences and the mass number of nuclei. This yields values of  $C_v(\rho_0)$  and  $C_s$  as  $32.1 \pm 0.31$  MeV and  $58.91 \pm 1.08$  MeV, respectively.

those found previously. Exploiting the empirical values of  $C_v(\rho_0)$  and  $C_s$ , an exploration was done earlier [38] with the ansatz given by Eq. (6) to calculate the equivalent density  $\rho_A$  for the 'benchmark' spherical nucleus  $^{208}\text{Pb}$  in the local density approximation [36]. Hereafter, we refer to the choice of Eq. (6) for the form of density dependence of  $C_v(\rho)$  as case I and the empirical values  $C_v(\rho_0)$  and  $C_s$  as  $C_v^0$  and  $C_s^0$  respectively.

The saturation density was chosen as  $\rho_0 = 0.155 \pm 0.008$  fm $^{-3}$ ; this covers the saturation densities that come out from the EOSs of different Skyrme and relativistic mean-field (RMF) models. The empirical information of the proton rms radius in  $^{208}\text{Pb}$  and the correlation of the symmetry slope parameter with the neutron skin thickness of  $^{208}\text{Pb}$ , all deduced from a family of RMF energy density functionals served to give a value of  $\gamma \sim 0.664 \pm 0.051$ , and hence  $L = 64 \pm 5$  MeV [38]. The neutron skin thickness for  $^{208}\text{Pb}$  is found to be  $0.188 \pm 0.014$  fm, the equivalent density  $\rho_A$ , comes out to be  $0.089$  fm $^{-3}$  from the model.

To confirm the robustness of the procedure adopted in our recent work [38], it is imperative to see whether choice of forms of density dependence of symmetry energy other than that given by Eq. (6) produce nearly the same results. It is also important to check if other heavy nuclei, spherical or otherwise, collate the conclusions arrived with this procedure. In the present communication we use different functional forms for the  $C_v(\rho)$ , employed very recently in Ref. [39, 40] in checking the validation of the relationship between  $C_v(\rho_0)$ ,  $L$  and  $K_{sym}$  using different effective interactions. Our calculations are performed for both the spherical and well deformed  $^{208}\text{Pb}$  and  $^{238}\text{U}$  nuclei, respectively. The density distribution of nucleons corresponding to different neutron-skin thickness, required for our calculations, are obtained using different energy density functionals based on the RMF model. The choices for these energy density functionals are exactly the same as in Ref. [38].

The form of  $C_v(\rho)$  given by Eq. (6) (case I) has some limitations [39]. With this functional form,  $C_v(\rho_0)$ ,  $L$  and  $K_{sym}$ , when calculated from Eqs. (1)–(3) can be correlated as,

$$C_v(\rho_0) = \frac{L}{3 + K_{sym}/L}. \quad (7)$$

The results for the relative error  $\Delta C_v/C_v$ , obtained using different RMF models, are displayed in Fig. 1. The  $\Delta C_v$  for the case I (black squares) is the difference in the lhs and rhs of Eq. (7). The values of  $C_v$ ,  $L$  and  $K_{sym}$  are calculated at  $\rho_0$  using Eqs. (1), (2) and (3), respectively. The departure of  $\Delta C_v/C_v$  from zero is indicative of the inaccuracy involved in expressing the functional dependence of symmetry energy as given by Eq. (6).

Another functional form for  $C_v(\rho)$  seems more pertinent [40]:

$$C_v(\rho) = C_k \left(\frac{\rho}{\rho_0}\right)^{2/3} + (C_v(\rho_0) - C_k) \left(\frac{\rho}{\rho_0}\right)^\gamma. \quad (8)$$

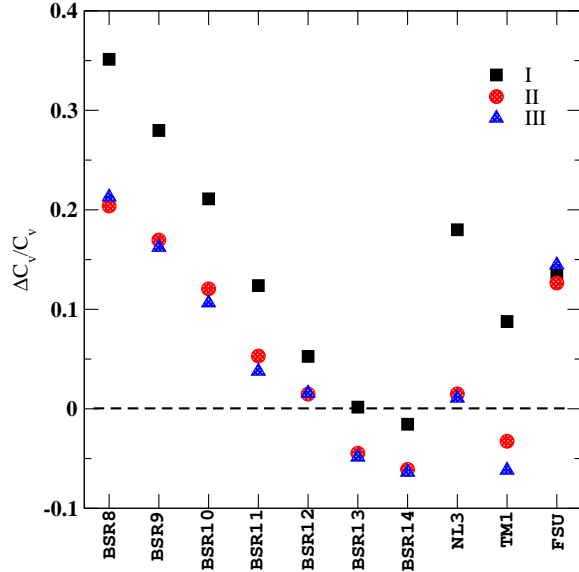


FIG. 1: (Color online) The relative error  $\Delta C_v/C_v$  calculated at  $\rho_0$  are shown for the various interactions pertaining to the cases I, II, and III. The meaning of the three cases are explained in the text.

The first term in the rhs of the above equation takes care of the kinetic energy contribution to the  $C_v(\rho)$ , the last term comes from interactions. The value of  $C_k$  is  $C_k = (2^{2/3} - 1) \times \frac{5}{3} \frac{P_{F,0}^2}{2m^*}$  where  $P_{F,0}$  is the Fermi momentum corresponding to the saturation density  $\rho_0$  and  $m^*$  is the nucleon effective mass.

Inspired by the density-dependent M3Y (DDM3Y) interaction, the density dependence of  $C_v(\rho)$  has also been shaped as [41],

$$C_v(\rho) = C_k \left(\frac{\rho}{\rho_0}\right)^{2/3} + C_1 \left(\frac{\rho}{\rho_0}\right) + C_2 \left(\frac{\rho}{\rho_0}\right)^{5/3}, \quad (9)$$

where  $C_2 = C_v(\rho_0) - C_1 - C_k$ . The density dependence of  $C_v(\rho)$  in the DDM3Y interaction, however, shows a different behavior as compared to the RMF models. Nevertheless, we use this functional form also to check the robustness of our calculations. The forms for  $C_v(\rho)$  depicted by Eqs. (8) and (9) are hereafter referred to as case II and case III. The three symmetry parameters are correlated as,

$$C_v(\rho_0) = C_k + \frac{(L - 2C_k)^2}{3L + K_{sym} - 4C_k}, \quad (10)$$

and

$$C_v(\rho_0) = \frac{L}{3} - \frac{K_{sym}}{15} + \frac{C_k}{5}, \quad (11)$$

for the cases II and III respectively. As seen in Fig. 1, the values of  $\Delta C_v(\rho_0)$  for cases II (red circles) and III (blue triangles) are quite similar for the interactions we have chosen; they lie closer to zero in comparison to those in

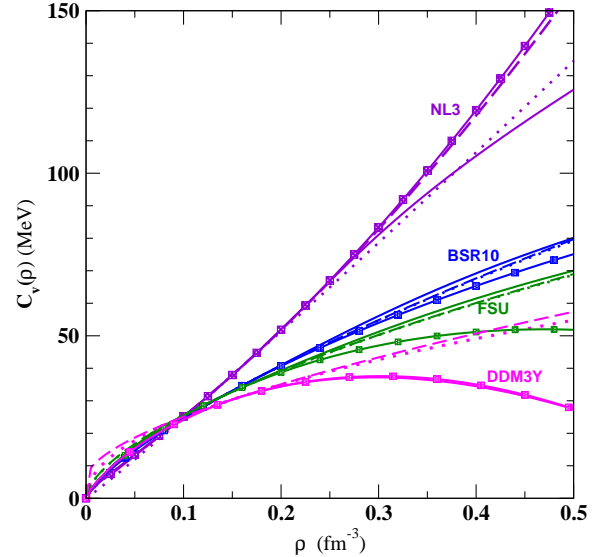


FIG. 2: (Color online) Symmetry energy plotted as a function of density for a few representative interactions. The lines in violet, blue, green and magenta colors correspond to NL3, BSR-10, FSU and DDM3Y interactions, respectively. The solid lines refer to  $C_v(\rho)$  calculated from Eq. (1), the dotted, dashed and lines with square symbols refer to case I, II and III, respectively. For the BSR10 and FSU, results for cases I and II overlap on each other. For the DDM3Y, result for case III is almost indistinguishable from the one calculated using Eq. (1).

From the above results, one can infer about the adequacy of the three functional forms for modeling the density dependence of the symmetry energy only at the saturation density. In Fig. 2, we plot the values of  $C_v(\rho)$  over a wide density range  $0 \leq \rho \leq 3\rho_0$  which are obtained using Eq. (1) for a few representative interactions. These values of  $C_v(\rho)$  are also compared with the ones obtained by fitting them to the cases I, II and III. In this density range, one sees that the symmetry energy has a stiff density dependence for NL3 [42] interaction, BSR10 [43] and FSU [7] display a softer dependence. All the three functional forms (Eqs. (6), (8), and (9)) are seen to give a moderately good representation of the density dependence of symmetry energy for the specific RMF interactions except at supranormal densities. For the DDM3Y interaction, it is seen that only case III (Eq. (9)) compares extremely well with  $C_v(\rho)$ . This is so because of construction.

To a good approximation,  $C_v(\rho)$  is given as [23]

$$C_v(\rho) = C_v(\rho_0) - L\epsilon + \frac{K_{sym}}{2}\epsilon^2 \quad (12)$$

where  $\epsilon = (\rho_0 - \rho)/3\rho_0$ . Since  $a_{sym}(A) = C_v(\rho_A)$ , one immediately gets, from Eqs. (4) and (12),

$$C_s = A^{1/3} \left[ L\epsilon_A - \frac{K_{sym}}{2}\epsilon_A^2 \right], \quad (13)$$

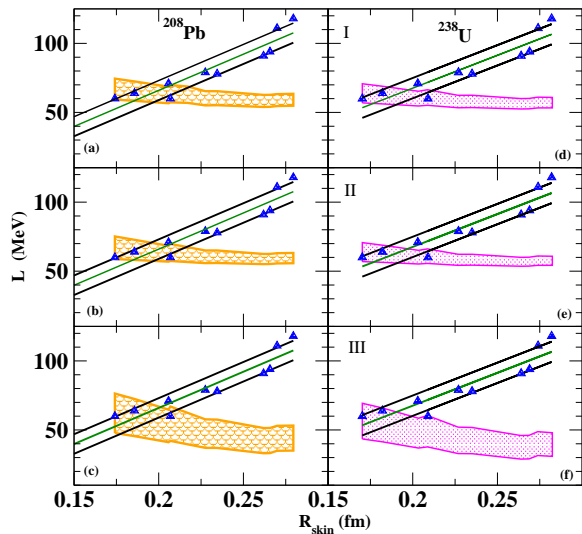


FIG. 3: (Color online) Symmetry slope parameter  $L$  calculated using Eq. (2) plotted as a function of  $R_{skin}$  of  $^{208}\text{Pb}$  and  $^{238}\text{U}$  evaluated with the different RMF interactions are shown by the blue triangles. The green lines with envelopes of slanted black lines refer to the least-squared fits to them with the spread-out error. The shaded regions in the left and right panels represent the envelope of possible  $L$  values calculated in case I, II and III. The intersection of the slanted envelopes and the shaded regions depict the acceptable window for the values of  $L$  and  $R_{skin}$  for the cases concerned.

$a_{sym}(A)(\equiv C_v(\rho_A))$ , in the local density approximation can be calculated as,

$$C_v(\rho_A) = \frac{1}{AX_0^2} \int d\mathbf{r} \rho(\mathbf{r}) C_v(\rho(\mathbf{r})) [X(\mathbf{r})]^2, \quad (14)$$

where  $X_0(= \frac{N-Z}{A})$  is the isospin asymmetry of the nucleus,  $\rho(\mathbf{r})$  is the sum of its neutron and proton densities and  $X(\mathbf{r})$  is the local isospin asymmetry. Once the neutron-proton density profiles in the nucleus are known, for case II say, with  $C_v(\rho)$  as given by Eq. (8), a chosen value of  $\gamma$  gives  $\rho_A$  and hence  $\epsilon_A$ . The symmetry slope parameter  $L$  and  $K_{sym}$  are obtained from the density derivative of  $C_v(\rho)$  as  $L = 2C_k + 3(C_v^0 - C_k)\gamma$ , the symmetry incompressibility  $K_{sym}$  is determined from Eq. (10) using this value of  $L$  and the input value of  $C_v(\rho_0)$  ( $=C_v^0$ ). Only when Eq. (13) is satisfied (with  $C_s = C_s^0$ ), one obtains the desired solution  $\gamma$ , thence  $L$ ,  $K_{sym}$  and  $\rho_A$ . These can, likewise be determined for Case I. In a similar fashion, for case III,  $C_1$  of Eq. (9) can be determined iteratively to give  $L = 5C_v^0 - 3C_k - 2C_1$  and  $K_{sym} = 10C_v^0 - 12C_k - 10C_1$ .

The procedure as described works best for heavy nuclei where volume effects predominate over surface effects. In Ref. [38], for case I,  $^{208}\text{Pb}$  was chosen as a representative nucleus. It usually serves as a benchmark for comparison with extracted bulk nuclear properties. The present calculations along with the spherical nucleus  $^{208}\text{Pb}$  are

to see if the extracted informations from the two nuclei are in consonance.

We have used the interactions BSR8-BSR14 [43], FSU [7], NL3 [42], and TM1 [44] to generate the neutron and proton density profiles of the two nuclei in the RMF model. These interactions in general reproduce many experimental bulk properties of finite nuclei and nuclear matter. The binding energies of  $^{208}\text{Pb}$  and  $^{238}\text{U}$  are obtained in close experimental agreement. The calculated values of the quadrupole deformation  $\beta_2 = 0.26 - 0.28$  for  $^{238}\text{U}$  from the various RMF models considered here agree very well with the experimental value  $\sim 0.29$ . The proton rms radii are also reproduced nearly exactly. There is a wide variation in the neutron rms radii, however; the calculated neutron skin thickness varies from  $\sim 0.17$  fm to  $\sim 0.28$  fm. In Fig. 3(a)-3(f), the symmetry energy slope parameters evaluated with these interactions using Eq. (2) are displayed as a function of the corresponding calculated  $R_{skin}$  (blue filled triangles) for  $^{208}\text{Pb}$  and  $^{238}\text{U}$ . For both the nuclei, an almost linear correlation of  $L$  with  $R_{skin}$  is observed. We also use Eqs. (6), (8), (9), (13), and (14) to calculate  $L$  from these functional forms (case I-III) by employing the microscopic nuclear densities for  $^{208}\text{Pb}$  and  $^{238}\text{U}$  obtained within the RMF models using the empirical constraints on the parameter sets  $C_v^0$  ( $=32.1 \pm 0.31$  MeV),  $C_s^0$  ( $=58.91 \pm 1.08$  MeV) and  $\rho_0$  ( $=0.155 \pm 0.008$  fm $^{-3}$ ). The so-calculated  $L$  values are depicted in the figures by a shaded region, the spread coming from the uncertainties in the values of  $C_v^0$ ,  $C_s^0$  and  $\rho_0$ . These values display an altogether different type of correlation of  $L$  with  $R_{skin}$ , the weak dependence coming from the imposed empirical constraints.

The change in  $L$  with  $R_{skin}$  as displayed by the filled triangles, after least-squares fitting, gives an almost linear correlation shown by the green straight lines passing through the triangles. The correlation coefficient for both  $^{208}\text{Pb}$  and  $^{238}\text{U}$  nuclei is 0.93. The small deviations from complete linearity yields the rms error on  $L$  values  $\sim 7.2$  MeV. The spread in the  $L$  values for a given neutron-skin thickness within the RMF models is contained within the slanted black lines in the Fig. 3. Their intersection with the shaded region projects out those value of neutron skin thickness for the nuclei concerned and also the density slope parameter  $L$  that are commensurate with the empirical windows for  $C_v^0$ ,  $C_s^0$  and  $\rho_0$ . The values of the symmetry slope parameter  $L$  and the neutron skin thickness  $R_{skin}$  for the two nuclei and the three cases are summarized in Table I. It is seen that for a particular functional form for  $C_v(\rho)$  (case I-III) chosen, the value of  $L$  is nearly independent of the heavy system. If results for all the three cases and the two nuclear systems are put together, the value of  $L$  spans the range  $59.0 \pm 13.0$  MeV. Case III, designed specifically for M3Y interaction shows a distinctly different behavior for  $C_v(\rho)$  at somewhat higher density beyond saturation as shown in Fig. 2. Remembering that in case II (as opposed to case I), the density dependence of the symmetry energy originating

TABLE I: The values of symmetry energy slope parameter  $L$  and the neutron-skin thickness  $R_{\text{skin}}$  obtained for different forms for the density dependence of  $C_v(\rho)$ , labelled as case I, II and III.

	$^{208}\text{Pb}$		$^{238}\text{U}$	
	L (MeV)	$R_{\text{skin}}$ (fm)	L (MeV)	$R_{\text{skin}}$ (fm)
Case I	64.8±7.2	0.195±0.022	62.5±6.2	0.192±0.022
Case II	64.1±6.8	0.196±0.021	62.2±6.8	0.191±0.021
Case III	58.2±11.7	0.193±0.018	56.0±10.0	0.184 ±0.014

it appears that case II is the most suitable choice for the functional form of  $C_v(\rho)$ . There is not much difference in the values of  $L$  deduced from the two cases though, this is because the exponent  $\gamma$  in case I is not much different from the density exponent in the symmetry kinetic energy. There is some confusion as to whether the effective nucleon mass  $m^*$  or the bare mass  $m$  should be used in evaluating  $C_k$ , we find that effects of interaction implicitly hidden in  $m^*$  are compensated by the corresponding change in  $\gamma$  so that the value of  $L$  is nearly unchanged.

In summary, building on the precise knowledge of the

volume and surface symmetry coefficients of nuclei and the nuclear saturation density, we have proposed a model that gives the value of the symmetry slope parameter  $L$  of infinite matter. The value of  $L$  so extracted is seen to be nearly independent of the choice of different forms of density dependence of symmetry energy and also the choice of heavy nuclei. The small uncertainties in the known empirical values of the volume and surface symmetry energy and the saturation density of nuclear matter keeps  $L$  in tight bounds. This helps in determining the nuclear EOS more accurately around the saturation density; prediction of the neutron skin thickness in narrower limits may further also help in having a better feel on the proper input in the isovector channel in the construction of energy density functionals.

### Acknowledgments

J.N.D acknowledges support of DST, Government of India. The authors gratefully acknowledge the assistance of Tanuja Agrawal in the preparation of the manuscript.

- 
- [1] W. D. Myers and W. J. Swiatecki, Ann. Phys. (N. Y.) **55**, 395 (1969).
- [2] W. D. Myers and W. J. Swiatecki, Nucl. Phys. **A336**, 267 (1980).
- [3] Peter Möller, William D. Myers, Heroic Sagawa, and Satoshi Yoshida, Phys. Rev. Lett. **108**, 052501 (2012).
- [4] B. A. Brown, Phys. Rev. Lett. **85**, 5296 (2000).
- [5] S. Typel and B. A. Brown, Phys. Rev. C **64**, 027302 (2001).
- [6] R. J. Furnstahl, Nucl. Phys. A **706**, 85 (2002).
- [7] B. G. Todd-Rutel and J. Piekarewicz, Phys. Rev. Lett. **95**, 122501 (2005).
- [8] P. Danielewicz *et al.*, Science, **298**, 1592 (2002).
- [9] A. W. Steiner, M. Prakash, J. M. Lattimer, and P. J. Ellis, Phys. Rep. **411**, 325 (2005).
- [10] H.-Th. Janka, K. Langanke, A. Marek, G. Martínez-Pinedo, and B. Müller, Phys. Rep. **442**, 38 (2007).
- [11] L. F. Roberts, G. Shen, V. Cirigliano, J. A. Pons, S. Reddy, and S. E. Woosley, Phys. Rev. Lett. **108** 061103 (2012).
- [12] A. W. Steiner, Phys. Rev. C **77**, 035805 (2008).
- [13] T. Sil *et al.*, Phys. Rev. C **71**, 045502 (2005).
- [14] D. H. Wen *et al.*, Phys. Rev. Lett. **103**, 211102 (2009).
- [15] A. Carbone, G. Colò, A. Bracco, L-G. Cao, P. F. Bortignon, F. Camera, and O. Wieland, Phys. Rev. C **81**, 041301 (R) (2010).
- [16] L. Trippa, G. Colò, and E. Vigezzi, Phys. Rev. C **77**, 061304 (R) (2008).
- [17] M. A. Famiano *et al.*, Phys. Rev. Lett. **97**, 052701 (2006).
- [18] D. V. Shetty, S. J. Yennello, and G. A. Souliotis, Phys. Rev. C **76**, 024606 (2007).
- [19] L. W. Chen, C. M. Ko, and B. A. Li, Phys. Rev. Lett. **94**, 032701 (2005)
- [20] B. A. Li, L. W. Chen, and C. M. Ko, Phys. Rep. **464**, 113 (2008).
- [21] L. W. Chen, Phys. Rev. C **83**, 044308 (2011).
- [22] A. W. Steiner and S. Gandolfi, Phys. Rev. Lett. **108**, 081102 (2012).
- [23] M. Centelles, X. Roca-Maza, X. Viñas, and M. Warda, Phys. Rev. Lett. **102**, 122502 (2009).
- [24] M. Warda, X. Viñas, X. Roca-Maza, and M. Centelles, Phys. Rev. C **80**, 024316 (2009).
- [25] A. Trzcińska *et al.*, Phys. Rev. Lett. **87**, 082501 (2001).
- [26] J. Jastrzebski *et al.*, Int. J. Mod. Phys. E **13**, 343 (2004).
- [27] A. Abrahamyan *et al.*, Phys. Rev. Lett. **108**, 112502 (2012).
- [28] C. J. Horowitz *et al.*, Phys. Rev. C **85**, 032501(R) (2012).
- [29] P.-G. Reinhard and W. Nazarewicz, Phys. Rev. C **81**, 051303(R) 2010.
- [30] J. Piekarewicz, Phys. Rev. C **83**, 034319 (2011).
- [31] A. Tammi *et al.*, Phys. Rev. Lett. **107**, 062502 (2011).
- [32] J. Piekarewicz, B. K. Agrawal, G. Colò, W. Nazarewicz, N. Paar, P.-G. Reinhard, X. Roca-Maza, and D. Vretenar, Phys. Rev. C **85**, 041302 (2012).
- [33] X. Roca-Maza, M. Brenna, B. K. Agrawal, P. F. Bortignon, G. Colò, Li-Gang Cao, N. Paar, and D. Vretenar, Phys. Rev. C **87**, 034301 (2013).
- [34] P. Danielewicz, Nucl. Phys. A **727**, 233 (2003).
- [35] M. Liu, N. Wang, Z. Li, and F. Zhang, Phys. Rev. C **82**, 064306 (2010).
- [36] S. K. Samaddar, J. N. De, X. Viñas, and M. Centelles, Phys. Rev. C **76**, 041602(R) (2007).
- [37] H. Jiang, G. J. Fu, Y. M. Zhao, and A. Arima, Phys. Rev. C **85**, 024301 (2012).

- [38] B. K. Agrawal, J. N. De, and S. K. Samaddar, Phys. Rev. Lett. **109**, 262501 (2012).
- [39] J. Dong, W. Zuo, J. Gu, and U. Lombardo, Phys. Rev. C **85**, 034308 (2012).
- [40] M. B. Tsang, Y. Zhang, P. Danielewicz, M. Famiano, Z. Li, W. G. Lynch, and A. W. Steiner, Phys. Rev. Lett. **102**, 122701 (2009).
- [41] T. K. Mukhopadhyay and D. N. Basu, Nucl. Phys. **A789**, 201 (2007).
- [42] G. A. Lalazissis, J. König, and P. Ring, Phys. Rev. C **55**, 540 (1997).
- [43] B. K. Agrawal, Phys. Rev. C **81**, 034323 (2010); S. K. Dhiman, R. Kumar, and B. K. Agrawal, Phys. Rev. C **76**, 045801 (2007).
- [44] Y. Sugahara and H. Toki, Nucl. Phys. **A579**, 557 (1994).